Published for SISSA by Springer

Received: July 12, 2017
Revised: September 29, 2017
Accepted: October 16, 2017
Published: October 24, 2017

Vector SIMP dark matter

Soo-Min Choi,[a] **Yonit Hochberg,**[b,c] **Eric Kuflik,**[b,c] **Hyun Min Lee,**[a] **Yann Mambrini,**[d] **Hitoshi Murayama**[e,f,g,h] **and Mathias Pierre**[d]

[a] *Department of Physics, Chung-Ang University, Seoul 06974, Korea*
[b] *Department of Physics, LEPP, Cornell University, Ithaca NY 14853, U.S.A.*
[c] *Racah Institute of Physics, Hebrew University of Jerusalem, Jerusalem 91904, Israel*
[d] *Laboratoire de Physique Théorique (UMR8627), CNRS, Univ. Paris-Sud, Université Paris-Saclay, 91405 Orsay, France*
[e] *Ernest Orlando Lawrence Berkeley National Laboratory, University of California, Berkeley, CA 94720, U.S.A.*
[f] *Department of Physics, University of California, Berkeley, CA 94720, U.S.A.*
[g] *Kavli Institute for the Physics and Mathematics of the Universe (WPI), University of Tokyo Institutes for Advanced Study, University of Tokyo, Kashiwa 277-8583, Japan*
[h] *Center for Japanese Studies, University of California, Berkeley, CA 94720, U.S.A.*

E-mail: soominchoi90@gmail.com, yonit.hochberg@gmail.com, ekuflik@gmail.com, hminlee@cau.ac.kr, yann.mambrini@th.u-psud.fr, hitoshi@berkeley.edu, mathias.pierre@th.u-psud.fr

Abstract: Strongly Interacting Massive Particles (SIMPs) have recently been proposed as light thermal dark matter relics. Here we consider an explicit realization of the SIMP mechanism in the form of vector SIMPs arising from an $SU(2)_X$ hidden gauge theory, where the accidental custodial symmetry protects the stability of the dark matter. We propose several ways of equilibrating the dark and visible sectors in this setup. In particular, we show that a light dark Higgs portal can maintain thermal equilibrium between the two sectors, as can a massive dark vector portal with its generalized Chern-Simons couplings to the vector SIMPs, all while remaining consistent with experimental constraints.

Keywords: Beyond Standard Model, Cosmology of Theories beyond the SM, Gauge Symmetry

ArXiv ePrint: 1707.01434

https://doi.org/10.1007/JHEP10(2017)162

JHEP10(2017)162

Contents

JHEP10(2017)162

1 Introduction

There is overwhelming evidence for the existence of dark matter (DM) in the Universe [1]. One of the most compelling particle physics candidates for dark matter is the Weakly Interacting Massive Particles (WIMPs). However, the absence of experimental signals in direct [2–5] and indirect [6, 7] detection experiments for WIMPs, has led researchers to focus attention in recent years on sub-GeV dark matter. Thermal production of such light dark matter is possible if, for instance, standard $2 \to 2$ annihilations proceed with small couplings [8] or if new annihilation mechanisms are present, such as $3 \to 2$ annihilations [9–11] or forbidden $2 \to 2$ channels [12, 13].

The thermal production of Strongly Interacting Massive Particles (SIMPs) [10] is based on freezeout of $3 \to 2$ self-annihilation of dark matter, with coupling between SIMPs and light Standard Model (SM) particles, which maintain kinetic equilibrium between the two sectors until freeze-out occurs. Various realizations of SIMP dark matter have been proposed in the literature, which often contain (pseudo)scalar dark matter particles with dark abelian or non-abelian gauge symmetries [10, 14–19]. Massive dark vector bosons can also be SIMP candidates when stemming from non-abelian dark gauge bosons [20–25],

as can be dark fermions or scalars when accompanied with a light dark photon or another scalar [26, 27]. Vector SIMP models are particularly predictive since the cubic and quartic self-interactions of dark matter are determined by a single gauge coupling. If the non-abelian dark gauge symmetry is spontaneously broken by the Higgs mechanism, the resulting massive dark Higgs can equilibrate the vector SIMPs and the SM via a Higgs portal coupling [20–22, 24, 28]. The spin information of the dark matter could be then be inferred from the invisible Higgs decay, as is the case for the WIMP [29].

In this paper, we consider vector SIMP dark matter in an $\mathrm{SU}(2)_X$ dark gauge theory, where the three massive (degenerate) $\mathrm{SU}(2)_X$ gauge bosons play the role of vector SIMPs. Equilibration between the dark and visible sectors can be achieved by elastic scattering between the dark matter and the $\mathrm{SU}(2)_X$ dark Higgs, provided that the latter is light enough to be thermalized with the SM via the Higgs portal until freeze-out occurs. As we will see, the dark Higgs can successfully thermalize the two sectors only when it is close in mass to the dark matter, in which case additional forbidden $2 \to 2$ annihilations are important as well. Alternatively, the dark $\mathrm{U}(1)_{Z'}$ photon can thermalize the dark and visible sectors via its kinetic mixing with the SM hypercharge alongside its coupling to the DM, which proceed through generalized Chern-Simons (CS) terms [30–35]. In both cases of the Higgs and vector portals, we find parameter space consistent with all existing constraints. Our results indicate that the framework can be probed via Higgs/Z-boson invisible decays as well as dark Higgs/dark photon searches in current and future collider and beam dump experiments.

This paper is organized as follows. We begin by describing the $\mathrm{SU}(2)_X$ dark gauge theory model in section 2, including the relevant Higgs and gauge-mixing vector portals to the SM. Section 3 discusses the $3 \to 2$ annihilation processes setting the DM abundance, the self-scattering cross sections, and the effects of forbidden channels on the relic density. Methods for achieving kinetic equilibrium between the dark and visible sectors via Higgs mixing and/or gauge mixing are addressed in section 4. We conclude in section 5.

2 The model

Here we present the framework for vector SIMPs: we start with the dark gauge theory, and then describe the Higgs interactions as well as kinetic gauge mixing and couplings between the dark photon and the dark matter.

2.1 The dark sector

We consider as a model for non-abelian SIMP dark matter an $\mathrm{SU}(2)_X$ gauge theory in the dark sector, broken completely due to the VEVs of a dark Higgs doublet Φ. The massive gauge bosons of $\mathrm{SU}(2)_X$, denoted by X^i_μ $(i = 1, 2, 3)$, are degenerate and stable due to a dark custodial isospin symmetry, and are a dark matter candidate [20, 21, 24]. The accidental custodial symmetry persists in the presence of the Higgs portal and Z' portal with the generalized Chern-Simons term which we discuss later, maintaining the stability of the dark matter.

JHEP10(2017)162

The Lagrangian for the dark sector is given by

$$\mathcal{L} = -\frac{1}{4}\vec{X}_{\mu\nu}\cdot\vec{X}^{\mu\nu} + \mathcal{L}_{\rm scalar}\,, \tag{2.1}$$

where the field strength tensors are $\vec{X}_{\mu\nu} = \partial_\mu\vec{X}_\nu - \partial_\nu\vec{X}_\mu + g_X(\vec{X}_\mu\times\vec{X}_\nu)$. The scalar potential is given by

$$\mathcal{L}_{\rm scalar} = |D_\mu\Phi|^2 + m_\Phi^2|\Phi|^2 - \lambda_\Phi|\Phi|^4\,, \tag{2.2}$$

with the covariant derivatives for the dark Higgs doublet is $D_\mu\Phi = (\partial_\mu - \frac{1}{2}ig_X\vec{\tau}\cdot\vec{X}_\mu)\Phi$.

After expanding the dark Higgs fields around the VEV as $\Phi = \frac{1}{\sqrt{2}}(0, v_X+\phi)^T$ in unitary gauge, one obtains gauge boson mass of $m_X = \frac{1}{2}g_X v_X$. The self-interactions of the vector dark matter and its interactions with the dark Higgs ϕ are given by

$$\begin{aligned}\mathcal{L} \supset & -\frac{1}{2}g_X(\partial_\mu\vec{X}_\nu - \partial_\nu\vec{X}_\mu)\cdot(\vec{X}^\mu\times\vec{X}^\nu) - \frac{1}{4}g_X^2(\vec{X}_\mu\cdot\vec{X}^\mu)^2 \\ & + \frac{1}{4}g_X^2(\vec{X}_\nu\cdot\vec{X}^\mu)(\vec{X}_\mu\cdot\vec{X}^\nu) + \frac{1}{2}m_X^2\vec{X}_\mu\cdot\vec{X}^\mu\left(\frac{2\phi}{v_X} + \frac{\phi^2}{v_X^2}\right)\,.\end{aligned} \tag{2.3}$$

The non-abelian interactions among the vector bosons X allow for $3\to 2$ annihilations as SIMPs. This idea is actually much more general than we discussed above. This symmetry breaking can also be considered as dynamical, as a result of chiral symmetry breaking $\mathrm{SU}(2)_L\times\mathrm{SU}(2)_R\to\mathrm{SU}(2)_V$ in an $\mathrm{SU}(N_c)$ gauge theory. This corresponds to the limit where $m_\phi\to\infty$ at low energies, while resonances can play an important role at higher energies. In this case, the coupling g_X is still considered perturbative.

Alternatively, we can consider the theory with a Higgs doublet in the strongly coupled regime $g_X \gg 1$. As pointed out by 't Hooft [36], an SU(2) gauge theory with a doublet scalar does not have an order parameter to distinguish the broken and confining phases, and hence the two phases are continuously connected, akin to liquid and gas phases of water at high pressures. In the strong coupling case, the vector SIMP is described by the interpolating field $\Phi^\dagger i\overset{\leftrightarrow}{D}_\mu\Phi$, while the dark Higgs by $\Phi^\dagger\Phi$. Given enough parameters in the model $(g_X, m_\Phi^2, \lambda_\Phi)$, one can most likely have the dark Higgs heavier than the vector SIMP as required (see below); such a discussion requires numerical simulations and is beyond the scope of this paper.

2.2 Higgs portal

The dark Higgs provides a portal between the dark sector and the visible sector, since the dark and SM scalars may interact at the renormalizable level,

$$\mathcal{L}_{\rm higgs} = \lambda_{\Phi H}|\Phi|^2|H|^2 + \lambda_{SH}|S|^2|H|^2 + \lambda_{\Phi S}|\Phi|^2|S|^2\,. \tag{2.4}$$

Here, a complex scalar field S is introduced for giving mass to Z' gauge boson by Higgs mechanism in the later discussion on Z' portal in section 2.3. Since Z' is assumed to be heavier than dark matter in our model, we assumed that the radial mode of S has no significant mixing with the dark Higgs ϕ and the SM Higgs.

JHEP10(2017)162

The SM and dark Higgs bosons are then mixed by

$$\begin{pmatrix} h_1 \\ h_2 \end{pmatrix} = \begin{pmatrix} \cos\theta & -\sin\theta \\ \sin\theta & \cos\theta \end{pmatrix} \begin{pmatrix} \phi \\ h \end{pmatrix} , \tag{2.5}$$

where h_1, h_2 are mass eigenstates of mass

$$m^2_{h_1,h_2} = \lambda_\Phi v_X^2 + \lambda_H v^2 \mp \sqrt{(\lambda_\Phi v_X^2 - \lambda_H v^2)^2 + \lambda^2_{\Phi H} v_X^2 v^2} \, , \tag{2.6}$$

and the mixing angle is given by

$$\tan 2\theta = \frac{\lambda_{\Phi H} v_X v}{\lambda_H v^2 - \lambda_\phi v_X^2} . \tag{2.7}$$

Here, we assume that the additional Higgs field s for $\mathrm{U}(1)_{Z'}$ is heavy enough so that its mixing effects with the above Higgs fields is negligible. The Higgs mixing yields interactions between the vector DM and the SM particles,

$$\begin{aligned} \mathcal{L} \supset & \frac{m_X^2}{v_X} \vec{X}_\mu \cdot \vec{X}^\mu (\cos\theta \, h_1 + \sin\theta \, h_2) + \frac{m_X^2}{2v_X^2} \vec{X}_\mu \cdot \vec{X}^\mu (\cos\theta \, h_1 + \sin\theta \, h_2)^2 \\ & - \frac{m_f}{v} \bar{f} f (-\sin\theta \, h_1 + \cos\theta \, h_2) \, , \end{aligned} \tag{2.8}$$

enabling communication between the two sectors.

In the presence of such Higgs-portal couplings, the SM Higgs can decay invisibly into a pair of dark gauge bosons or dark higgses, with decay rates

$$\begin{aligned} \Gamma(h_2 \to XX) &= \frac{3\sin^2\theta m_{h_2}^3}{32\pi v_X^2} \left(1 - \frac{4m_X^2}{m_{h_2}^2} + \frac{12 m_X^4}{m_{h_2}^4}\right) \sqrt{1 - \frac{4m_X^2}{m_{h_2}^2}} \, , \\ \Gamma(h_2 \to h_1 h_1) &= \frac{\lambda^2_{\Phi H} v^2}{32\pi m_{h_2}} \sqrt{1 - \frac{4m_{h_1}^2}{m_{h_2}^2}} \, . \end{aligned} \tag{2.9}$$

The visible decays of the SM Higgs are scaled down universally by $\cos^2\theta$ due to the Higgs mixing. As we will see in section 4.2, the bound on invisible Higgs decays places a strong constraint on the allowed mixing, and hence on the possibility that the Higgs portal maintains kinetic equilibrium between the two sectors.

2.3 Vector portal

In addition to the Higgs portal, we can gauge a $\mathrm{U}(1)_{Z'}$ symmetry acting on the complex scalar S, with the covariant derivative $D_\mu S = (\partial_\mu - i g_{Z'} Z'_\mu) S$. The $\mathrm{U}(1)_{Z'}$ massive gauge boson Z' can connect the dark and visible sectors, in the presence of gauge kinetic mixing with the SM hypercharge as well as DM-Z' interactions:

$$\mathcal{L}_{\text{vector}} = -\frac{1}{2} \sin\xi \, Z'_{\mu\nu} B^{\mu\nu} + \mathcal{L}_{XXZ'} \, . \tag{2.10}$$

Here $\mathcal{L}_{XXZ'}$ generates a 3-pt interaction between XXZ'; it may be generated by a non-abelian Chern-Simons (CS) term, as will be discussed below.

JHEP10(2017)162

The kinetic and mass terms for the Z and Z' gauge bosons [15] is diagonalized

$$\begin{pmatrix} B_\mu \\ W^3_\mu \\ Z'_\mu \end{pmatrix} = \begin{pmatrix} c_W & -s_W c_\zeta + t_\xi s_\zeta & -s_W s_\zeta - t_\xi c_\zeta \\ s_W & c_W c_\zeta & c_W s_\zeta \\ 0 & -s_\zeta/c_\xi & c_\zeta/c_\xi \end{pmatrix} \begin{pmatrix} A_\mu \\ Z_{1\mu} \\ Z_{2\mu} \end{pmatrix} \tag{2.11}$$

where (B_μ, W^3_μ, Z'_μ) are hypercharge, neutral-weak and dark gauge fields, $(A_\mu, Z_{1\mu}, Z_{2\mu})$ are mass eigenstates, and $s_W \equiv \sin\theta_W, c_W \equiv \cos\theta_W$, etc. Here, Z_1 is Z-boson-like and Z_2 is Z'-boson-like, with masses

$$m^2_{1,2} = \frac{1}{2}\left[m^2_Z(1+s^2_W t^2_\xi) + m^2_{Z'}/c^2_\xi \pm \sqrt{(m^2_Z(1+s^2_W t^2_\xi)+m^2_{Z'}/c^2_\xi)^2 - 4m^2_Z m^2_{Z'}/c^2_\xi}\right], \tag{2.12}$$

where the mixing angle is

$$\tan 2\zeta = \frac{m^2_Z s_W \sin 2\xi}{m^2_{Z'} - m^2_Z(c^2_\xi - s^2_W s^2_\xi)}\,. \tag{2.13}$$

The electromagnetic and neutral-current interactions are then

$$\begin{aligned} \mathcal{L}_{\rm EM/NC} = {} & eA_\mu J^\mu_{\rm EM} + Z_{1\mu}\left[e\varepsilon J^\mu_{\rm EM} + \frac{e}{2s_W c_W}(c_\zeta - t_W\varepsilon/t_\zeta)J^\mu_Z - g_{Z'}\frac{s_\zeta}{c_\xi}J^\mu_{Z'}\right] \\ & + Z_{2\mu}\left[-e\varepsilon J^\mu_{\rm EM} + \frac{e}{2s_W c_W}(s_\zeta + t_W\varepsilon)J^\mu_Z + g_{Z'}\frac{c_\zeta}{c_\xi}J^\mu_{Z'}\right], \end{aligned} \tag{2.14}$$

where $\varepsilon \equiv c_W t_\xi c_\zeta \simeq c_W\xi$ for $|\xi| \ll 1$, and $J^\mu_{\rm EM}$, J^μ_Z and $J^\mu_{Z'}$ are electromagnetic, neutral and dark currents, respectively. For $m_{Z'} \ll m_Z$, one has $\zeta \simeq -s_W\xi = -t_W\varepsilon$, so the neutral current interaction of the dark photon is negligible due to $s_\zeta + t_W\varepsilon \simeq \zeta + s_W\xi \simeq 0$.

There are no direct couplings between the SM and the non-abelian vector dark matter at the renormalizable level, because of the non-abelian gauge symmetry. Likewise, there are no direct renormalizable interactions between the Z' and the X-boson, since the dark Higgs are not charged under both symmetries (in other words, the dark Weinberg angle vanishes).

If heavy fermions charged under both $\mathrm{SU}(2)_X$ and $\mathrm{U}(1)_{Z'}$ are present in the theory, they may generate low-energy effective XXZ' interactions via triangle diagrams. From the effective theory point of view these may manifest as generalized non-abelian Chern-Simons terms [33, 34],

$$\mathcal{L}_{\rm CS,EFT} \supset c_1\epsilon^{\mu\nu\rho\sigma}Z'_\mu\vec{X}_\nu\cdot(\partial_\rho\vec{X}_\sigma - \partial_\sigma\vec{X}_\rho)\,. \tag{2.15}$$

Although the coefficient c_1 is dimensionless, these are non-renormalizable operators and arise from gauge dimension-8 operators, known as D'Hoker-Farhi terms [37],

$$\mathcal{L}_{\rm CS} \supset \frac{i}{M^4}S^\dagger D^\mu S(D^\nu\Phi)^\dagger\tilde{X}_{\mu\nu}\Phi + \text{c.c.} \tag{2.16}$$

Likewise, an effective 3-pt interaction can be generated by the gauge invariant dimension-8 operator of the form

$$\mathcal{L}_{D8} = \frac{1}{M^4}\,\epsilon^{\mu\nu\rho\sigma}(\Phi^\dagger X_{\mu\nu}D_\lambda\Phi)\partial^\lambda Z'_{\rho\sigma}\,. \tag{2.17}$$

JHEP10(2017)162

In this work we will consider the phenomenology of the effective operator eq. (2.15); appendix A contains a concrete example of generating the effective Chern Simons term.

We remark on the invisible decays of Z and Z' bosons in our setup. The Z boson can decay invisibly into a pair of vector dark matter particles through the generalized CS terms in the presence of a gauge kinetic mixing between Z' and Z bosons. But, if N_f heavy fermions f running in triangle diagrams are relatively light for a sizable CS term (but heavy enough not to affect our discussion on vector SIMPs in the later sections) as discussed in appendix A, the Z-boson preferentially decays directly into a pair of heavy fermions at tree level. Then, the corresponding Z-boson invisible decay width is given by

$$\Gamma(Z_1 \to f\bar{f}) = \frac{N_f \alpha_{Z'} \varepsilon^2 m_Z}{3c_W^2} \left(1 + \frac{2m_f^2}{m_{Z'}^2}\right) \left(1 - \frac{4m_f^2}{m_Z^2}\right)^{1/2} \tag{2.18}$$

with $\alpha_{Z'} \equiv g_{Z'}^2/(4\pi)$. On the other hand, if the heavy fermions are heavier than $m_{Z'}/2$, the Z' boson decays into a pair of vector dark matter particles via the CS term, with the width

$$\Gamma(Z_2 \to XX) = \frac{c_1^2 m_{Z'}^3}{8\pi m_X^2} \left(1 - \frac{4m_X^2}{m_{Z'}^2}\right)^{5/2} . \tag{2.19}$$

3 Vector SIMP dark matter

Having established the interactions of the framework, we now address the cross section for the dark matter relic abundance and self-scatterings. We first determine the relic density of dark matter from $3 \to 2$ processes in section 3.1, and discuss the role of additional forbidden annihilation channels in section 3.2.

3.1 SIMP channels

Here we compute the relic density assuming the $3 \to 2$ annihilation processes are the dominant number-changing processes. In the presence of an isospin symmetry for the vector dark matter, all components of dark matter have the same mass, and can be treated as identical particles. Assuming the dark matter remains in kinetic equilibrium with the SM until the time of freeze-out, the Boltzmann equation for the vector dark matter is given by [10]

$$\begin{aligned} \frac{dn_{\rm DM}}{dt} + 3Hn_{\rm DM} = &-\Big(\langle\sigma v^2\rangle_{3\to2} - \langle\sigma v^2\rangle_{3\to2}^h\Big)\Big(n_{\rm DM}^3 - n_{\rm DM}^2 n_{\rm DM}^{\rm eq}\Big) \\ &- \langle\sigma v^2\rangle_{3\to2}^h\Big(n_{\rm DM}^3 - n_{\rm DM}(n_{\rm DM}^{\rm eq})^2\Big) . \end{aligned} \tag{3.1}$$

Here, the thermally averaged $3 \to 2$ annihilation cross-section (away from a resonance) is given by

$$\begin{aligned} \langle\sigma v^2\rangle_{3\to2} = &\frac{25\sqrt{5}g_X^6}{23887872\pi m_X^5} \frac{1}{(m_{h_1}^2 - 4m_X^2)^2(m_{h_1}^2 + m_X^2)^2}\Big(14681m_{h_1}^8 - 87520m_{h_1}^6 m_X^2 \\ &+ 21004m_{h_1}^4 m_X^4 + 327580m_{h_1}^2 m_X^6 + 290775m_X^8\Big) + \langle\sigma v^2\rangle_{3\to2}^h \end{aligned} \tag{3.2}$$

JHEP10(2017)162

with

$$\langle\sigma v^2\rangle^h_{3\to2} = \frac{\sqrt{5}g_X^6 m_{h_1}^{16}}{80621568\pi m_X^{10}} \frac{(1-m_{h_1}^2/(16m_X^2))^{1/2}}{(m_{h_1}^2-4m_X^2)^{7/2}(m_{h_1}^2+2m_X^2)^2}\left(C_1+\frac{2C_2 m_{h_1}^4}{(m_{h_1}^2-7m_X^2)^2}\right) \tag{3.3}$$

where C_1 and C_2 are dimensionless quantities given in eqs. (B.12) and (B.14), respectively. We note that the first term in $\langle\sigma v^2\rangle_{3\to2}$ stems from $XXX \to XX$ channels and $\langle\sigma v^2\rangle^h_{3\to2}$ due to $XXX \to Xh_1$ channels contributes only for $m_{h_1} < 2m_X$, becoming dominant near the resonance at $m_{h_1} = 2m_X$. On the other hand, $XXX \to h_1h_1$ channels are p-wave suppressed so they are not included here. Additional terms that give an approximate resonance when $m_{h_1} = 3m_X$ are present, but as they are p-wave suppressed they are always subdominant and hence can be neglected. Further details of the $3 \to 2$ cross section and discussion of the Boltzmann equation can be found in appendix B.

In the instantaneous freeze-out approximation, the relic abundance for $3 \to 2$ annihilation is found to be

$$\Omega_{\rm DM} \simeq \frac{m_X s_0/\rho_c}{s(m_X)^2/H(m_X)} \frac{x_f^2}{\sqrt{\langle\sigma v^2\rangle_{3\to2}}}\,, \tag{3.4}$$

where $s_0/\rho_c \simeq 6\cdot 10^8/\text{GeV}$ is the ratio of the entropy density today to the critical density, $s(m_X)$ is the entropy density at $T = m_X$, and $H(m_X)$ is the Hubble rate at $T = m_X$. Here $x_f = m_X/T_f$ indicates the freezeout temperature, which is typically $x_f \in [15, 20]$ for $3 \to 2$ freezeout. For $m_{h_1} \gtrsim 3m_X$, the Higgs contributions to the cross-section effectively decouples, and we have

$$\Omega_{\rm DM} \simeq 0.33\left(\frac{x_f}{20}\right)^2\left(\frac{10.75}{g_*}\right)^{3/4}\left(\frac{m_X/\alpha_X}{100\,\text{MeV}}\right)^{3/2}. \tag{3.5}$$

In figure 1 we depict the parameter space in which the measured dark matter relic density is obtained within 3σ (red region) for $\alpha_X \equiv g_X^2/(4\pi)$ (m_{h_1}) and m_X in the upper (lower) panel. For illustration, the top panel shows the results for dark Higgs mass of $m_{h_1} = 4m_X$ where no resonance enhancement is present, while in the bottom panel we fix $\alpha_X = 1, 2$ and vary m_X and m_{h_1}.

In addition to $3 \to 2$ annihilations, the vector SIMP dark matter undergoes self-scattering processes, which are constrained by the bullet cluster [38–40] and by elliptical halo shapes [41, 42]. Away from a resonance, the self interacting cross-section is

$$\begin{aligned}\sigma_{\rm self} = \frac{g_X^4}{1152\pi m_{h_1}^4 m_X^2(m_{h_1}^2-4m_X^2)^2}\Big(&520m_{h_1}^8 - 4208m_{h_1}^6 m_X^2 + 8801m_{h_1}^4 m_X^4 \\ &- 1200m_{h_1}^2 m_X^6 + 320m_X^8\Big)\,.\end{aligned} \tag{3.6}$$

A simple approximation can be derived in the limit $m_{h_1} \gg m_X$:

$$\frac{\sigma_{\rm self}}{m_X} \simeq \frac{65\pi\alpha_X^2}{9m_X^3} \simeq 5\alpha_X^2\left(\frac{m_X}{100\text{ MeV}}\right)^{-3}\text{cm}^2/\text{g} \qquad [m_{h_1} \gg m_X] \tag{3.7}$$

Contours of the self-scattering cross section obeying $\sigma_{\rm self}/m_X = 0.1, 1, 10\,\text{cm}^2/\text{g}$ are shown in figure 1 in dotted, dashed and dot-dashed lines, respectively.

JHEP10(2017)162

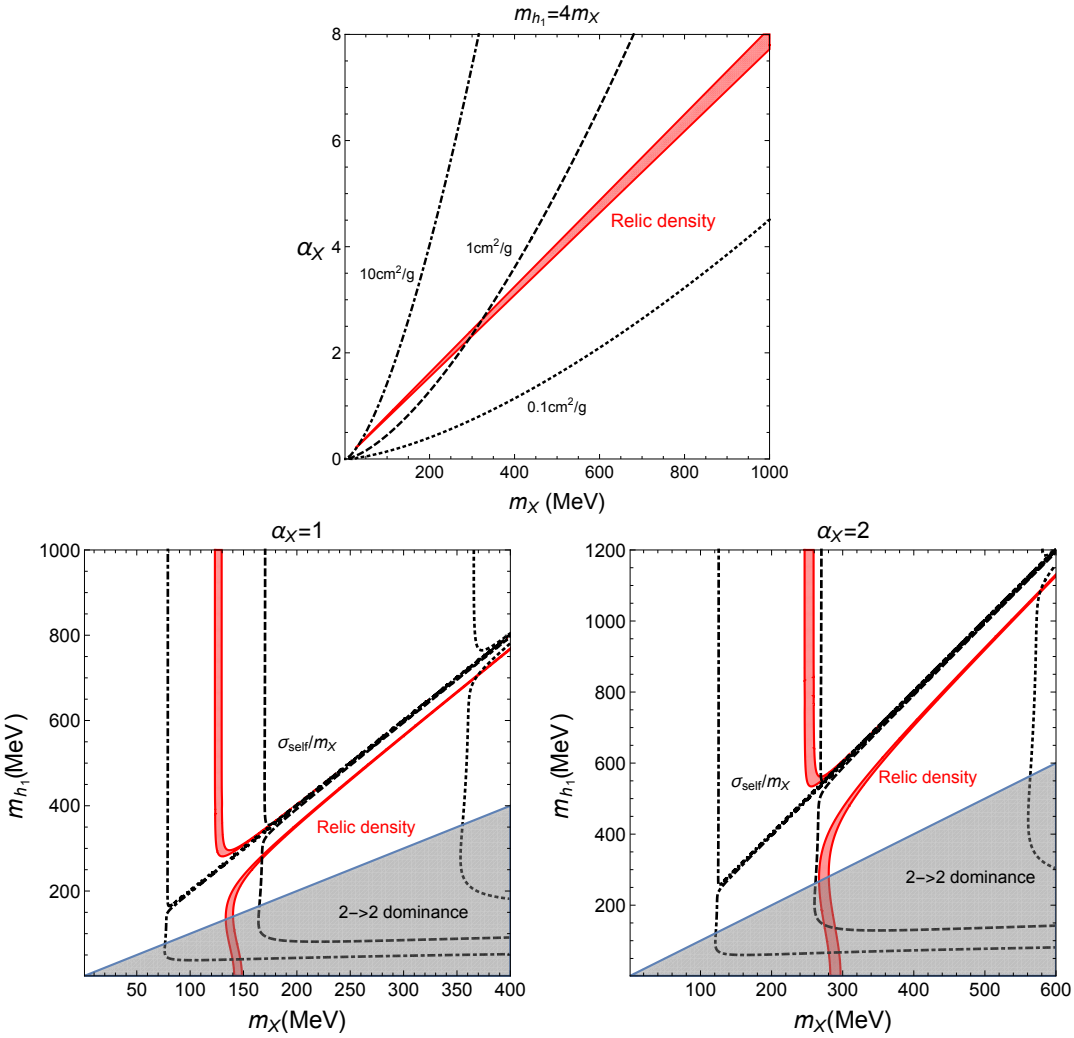

Figure 1. The parameter space of vector SIMP dark matter in the m_X vs. $\alpha_X \equiv g_X^2/(4\pi)$ (top) or m_{h_1} (bottom), when considering $3 \to 2$ annihilation channels only. The Planck 3σ measurement of the relic density is show in red in all panels. Contours of the self-scattering cross section of $\sigma_{\rm self}/m_X = 0.1, 1, 10\,{\rm cm}^2/{\rm g}$ are shown in the dotted, dashed and dot-dashed curves, respectively. We have chosen $m_{h_1} = 4m_X$ on top and $\alpha_X = 1, 2$ on bottom. The shaded gray regions in the lower panels are where other $2 \to 2$ channels dominate over $3 \to 2$ processes.

We learn that away from a resonance region, vector SIMP $3 \to 2$ dark matter consistent with self-scattering constraints points to dark matter masses of $m_X \gtrsim \mathcal{O}(100\,{\rm MeV})$ and strong couplings of $\alpha_X \gtrsim 1$. Indeed, strong coupling is a frequent common feature in SIMP dark matter models [10, 14–16, 18, 20, 21, 24, 26], though exceptions can arise (e.g. on resonance [17, 19]). Close to the resonance region, the relic density is sensitive to the dark Higgs mass, and the viable parameter space is broadened further to include larger DM masses at fixed dark gauge coupling, or smaller dark gauge couplings for fixed DM masses.

We comment that the strong gauge coupling leads to a question on the potential breakdown of perturbativity in relic density calculation. In our case, however, the $\mathrm{SU}(2)_X$

JHEP10(2017)162

gauge symmetry is completely broken by the VEV of the dark Higgs, and there are no light particles below the confinement or symmetry breaking scale (i.e., vector SIMP mass). Therefore, given that there is no phase transition separating the Higgs phase and confining phase, namely, the complementarity between the Higgs and confining phases [36, 43–47], the Higgsed theory can be pushed into regions where perturbativity is questionable. Closer inspection of the issue of complementarity may be worthwhile, though is beyond the scope of this paper.

As the dark Higgs mass approaches the DM mass, when $m_X < m_{h_1} \lesssim 1.5 m_X$, forbidden $2 \to 2$ annihilation channels contribute significantly to the relic density and must be included as well; we study this in the next subsection. (The regions in which $2 \to 2$ processes dominate the relic density are shown in shaded gray in figure 1.) As we will see, the self-scattering rate is reduced in this case, allowing smaller dark matter masses consistent with observational constraints.

3.2 Forbidden channels

When the dark Higgs is slightly heavier than the dark matter, forbidden $2 \to 2$ channels such as $X_i X_i \to h_1 h_1$ and $X_i X_j \to X_k h_1$ — although kinematically inaccessible at zero temperature — can be important in determining the relic density at the time of freeze-out [12, 13]. For $m_X \lesssim m_{h_1} \lesssim 2(1.5) m_X$, new $3 \to 2$ channels such as $XXX \to X h_1 (h_1 h_1)$ open up as well so they have been already included in figure 1. Here we discuss the effects of the forbidden channels on the relic abundance and identify the parameter space of vector SIMP dark matter that is consistent with the observed relic density when including these effects. (This will be particularly relevant when kinetic equilibrium between the SIMP and SM sectors is obtained via the Higgs portal, as will become evident in section 4.2.)

Assuming that the forbidden channels are dominant, the approximate Boltzmann equation is given by

$$\begin{aligned} \frac{dn_{\rm DM}}{dt} + 3Hn_{\rm DM} \approx & -\frac{2}{3}\langle\sigma v\rangle_{ii\to h_1 h_1} n_{\rm DM}^2 + 6\langle\sigma v\rangle_{h_1 h_1 \to ii} (n_{h_1}^{\rm eq})^2 \\ & - \frac{1}{3}\langle\sigma v\rangle_{ij\to k h_1} n_{\rm DM}^2 + \langle\sigma v\rangle_{k h_1 \to ij} n_{h_1}^{\rm eq} n_{\rm DM} \,, \end{aligned} \tag{3.8}$$

where we have assumed that h_1 maintains chemical and thermal equilibrium with the SM bath throughout freezeout. See the full Boltzmann equations in eq. (B.15). Detailed balance conditions at high temperature determine the annihilation cross sections for the forbidden channels in terms of the unforbidden channels,

$$\langle\sigma v\rangle_{ii\to h_1 h_1} = \frac{9(n_{h_1}^{\rm eq})^2}{(n_{\rm DM}^{\rm eq})^2} \langle\sigma v\rangle_{h_1 h_1 \to ii} = (1+\Delta_{h_1})^3 e^{-2\Delta_{h_1} x} \langle\sigma v\rangle_{h_1 h_1 \to ii} \,, \tag{3.9}$$

$$\langle\sigma v\rangle_{ij\to k h_1} = \frac{3 n_{h_1}^{\rm eq}}{n_{\rm DM}^{\rm eq}} \langle\sigma v\rangle_{k h_1 \to ij} = (1+\Delta_{h_1})^{3/2} e^{-\Delta_{h_1} x} \langle\sigma v\rangle_{k h_1 \to ij} \,, \tag{3.10}$$

with $\Delta_{h_1} \equiv (m_{h_1} - m_\chi)/m_\chi$. The cross section formulas for the allowed $2 \to 2$ channels in the r.h.s. above are given in appendix B.

JHEP10(2017)162

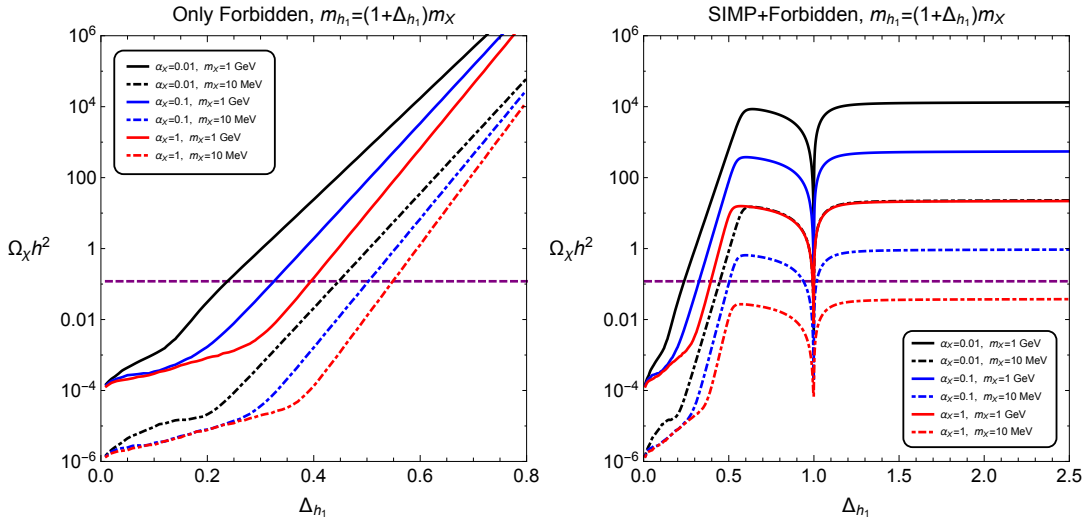

Figure 2. Dark matter relic density as a function of $\Delta_{h_1} = (m_{h_1} - m_X)/m_X$, for forbidden channels only (*left*) and both forbidden and SIMP channels (*right*). The measured relic density is shown by the purple curve. We show the results for various illustrative values of coupling and mass: $\alpha_X = 0.01, 0.1, 1$ and $m_X = 0.1\,\text{MeV}, 1\,\text{GeV}$.

Denoting the allowed $2 \to 2$ cross sections in the r.h.s. above by $\langle\sigma v\rangle_{kh_1\to ij} = a$ and $\langle\sigma v\rangle_{h_1h_1\to ii} = b$, the DM abundance is found to be [13]

$$Y_{\rm DM}(\infty) \approx \frac{x_f}{\lambda}\, e^{\Delta_{h_1} x_f}\, f(\Delta_{h_1}, x_f) \tag{3.11}$$

with

$$f(\Delta_{h_1}, x_f) = \left[\frac{1}{3}a(1+\Delta_{h_1})^{3/2}\left(1 - (\Delta_{h_1}x_f)\, e^{\Delta_{h_1}x_f}\int_{\Delta_{h_1}x_f}^{\infty} dt\, t^{-1}e^{-t}\right)\right. \tag{3.12}$$
$$\left. + \frac{2}{3}b(1+\Delta_{h_1})^3 e^{-\Delta_{h_1}x_f}\left(1 - 2(\Delta_{h_1}x_f)\, e^{2\Delta_{h_1}x_F}\int_{2\Delta_{h_1}x_f}^{\infty} dt\, t^{-1}e^{-t}\right)\right]^{-1},$$

resulting in the relic density

$$\Omega_{\rm DM}h^2 = 5.20\times 10^{-10}\,\text{GeV}^{-2}\left(\frac{g_*}{10.75}\right)^{-1/2}\left(\frac{x_f}{20}\right) e^{\Delta_{h_1}x_f} f(\Delta_{h_1}, x_f)\,. \tag{3.13}$$

In general, however, one must account simultaneously for both the $3 \to 2$ processes and the $2 \to 2$ forbidden channels in determining the dark matter relic abundance.

In figure 2, we show the dark matter relic density as a function of $\Delta_{h_1}=(m_{h_1}-m_X)/m_X$, first when including only forbidden channels (*left panel*) and then when taking both forbidden and SIMP channels into account (*right panel*). We have varied α_X and m_X between 0.01–1 and 10 MeV–1 GeV, respectively. We learn that forbidden channels play an important role for $\Delta_{h_1} \lesssim 0.5$, where the observed relic density can be achieved over a broad range of couplings α_X and masses m_X. As the mass difference increases, $3 \to 2$ SIMP annihilations begin dominating the relic abundance as a saturated value for mass differences

JHEP10(2017)162

$\Delta_{h_1} \gtrsim 0.5$. We note that the importance of the forbidden semi-annihilation channels for $\Delta_{h_1} \lesssim 0.5$, in contrast to the naive expectation from the Boltzmann suppression factors of $\Delta_{h_1} \lesssim 1$, is due to a large numerical factor in the SIMP $3 \to 2$ annihilation cross section.

4 Kinetic equilibrium

In order of the SIMP mechanism to be viable, we require that the SIMP sector efficiently dumps entropy into the SM bath. In the proposed framework, this can be achieved either by a Higgs or Z' portal between the vector SIMPs and SM particles. After a general discussion of the relevant Boltzmann equation in terms of the dark sector temperature and the requirement of equilibration in section 4.1, we study the Higgs portal in section 4.2 and the Z' portal in section 4.3.

4.1 Equilibration conditions

Following ref. [48], we find the decoupling temperature by comparing the rate of change in kinetic energy injected by the $3 \to 2$ annihilations compared to the kinetic energy lost due to elastic scattering. When the $3 \to 2$ occurs, the mass of one dark particle is converted to the kinetic energy of the 2 outgoing particles. These particles quickly scatter off the dark matter particles, and distribute the energy to the dark bath. Thus, the $3 \to 2$ annihilations maintain chemical equilibrium in the DM gas, while releasing kinetic energy per particle

$$\dot{K}_{3\to 2} = m_{\rm DM} \frac{\dot{n}_{\rm DM}}{n_{\rm DM}} \simeq -m_{\rm DM}^2 H T^{-1}. \tag{4.1}$$

Elastic scattering processes transfer this excess kinetic energy to the SM gas at a rate

$$\dot{K}_{\rm el} = \frac{1}{2E_p} \sum_i \frac{g_i d^3k_i}{(2\pi)^3 2E_i} \frac{d^3k_i'}{(2\pi)^3 2k_i'} \frac{d^3p'}{(2\pi)^3 2p'} \delta^4(p + k_i - p' - k_i') \overline{|\mathcal{M}|^2} \left(E_p - E_{p'}\right). \tag{4.2}$$

Here, the sum is taken over the species i in the relativistic plasma with initial(final) momentum $k(k')$, $p(p')$ is the dark matter initial(final) momentum. In the limit of $|\vec{k}| \ll m_{\rm DM}$, the change in kinetic energy can be written in terms of the momentum relaxation rate, $\gamma(T)$

$$\dot{K}_{\rm el} \simeq T\gamma(T) = \sum_i \frac{g_i}{6m_{\rm DM}} \int_0^\infty \frac{d^3\vec{k}}{(2\pi)^3} f_i(1 \pm f_i) \frac{|\vec{k}|}{\sqrt{\vec{k}^2 + m_i^2}} \int_{-4k^2}^0 dt(-t) \frac{d\sigma_{Xi\to Xi}}{dt}, \tag{4.3}$$

where t is the squared momentum transfer between DM and the relativistic species. The differential elastic scattering cross section is given by

$$\frac{d\sigma_{Xi\to Xi}}{dt} = \frac{1}{64\pi m_{\rm DM}^2 k^2} \overline{|\mathcal{M}_{Xi\to Xi}|^2}. \tag{4.4}$$

The decoupling occurs when the DM-to-SM energy transfer can no longer keep up with the kinetic energy production; equating eq. (4.1) with eq. (4.3), we have

$$\gamma(T_{\rm KD}) \simeq H(T_{\rm KD}) \frac{m_{\rm DM}^2}{T_{\rm KD}^2}, \tag{4.5}$$

JHEP10(2017)162

where $H = 0.33 g_*^{1/2} T^2/M_{\rm Pl}$ with $g_* = 10.75$ the effective relativistic number of species for $1\,\text{MeV} \lesssim T \lesssim 100\,\text{MeV}$ and $M_{\rm Pl} = 2 \times 10^{18}\,\text{GeV}$ the Planck scale. In what follows we use eq. (4.5), evaluated at $T_{\rm KD} = m_{\rm DM}/20$, to place a lower bound on the interactions between the vector SIMPs and the SM particles, needed to achieve the correct DM abundance. The ELDER DM curve [48, 49], corresponds to $T_{\rm KD} \simeq m_{\rm DM}/15$, where the relic abundance is determined by the elastic scattering rate.

The dark matter can also thermalize with the SM, if the dark matter maintains equilibrium with the dark Higgs, while the dark Higgs maintains equilibrium with the SM bath via decay and inverse decays into SM fermions. The dark Higgs should be heavier than the dark X-bosons, or else the dark matter will efficiently annihilate into dark Higgs, effectively becoming a WIMP-like scenario. However, if the dark Higgs is much heavier than the dark matter, then the dark Higgs abundance will have been sufficiently depleted and it will not be able to maintain equilibrium between the two sectors. This pushes the spectrum to a forbidden regime, $m_X < m_{h_1} \lesssim 1.5 m_X$, where the dark matter can annihilate into dark Higgses, but with a large Boltzmann suppression. At the time right before freezeout, both the semi-annihilation $XX \to X h_1$ and self-annihilation $XXX \to XX$ processes will be active for large gauge coupling. The dark sector will be in thermal equilibrium with vanishing chemical potential. Thus in order for freezeout to occur one just needs to check that the dark Higgs can deplete the density in the dark sector fast enough up until freezeout,

$$n_{h_1}^{\rm eq}(T_{\rm FO}) \Gamma_{h_1 \to \rm SM} > H(T_{\rm FO}) \left[n_X^{\rm eq}(T_{\rm FO}) + n_{h_1}^{\rm eq}(T_{\rm FO}) \right] . \tag{4.6}$$

We use the above condition on the dark Higgs decay rate in the case that vector SIMPs are in kinetic equilibrium through the scattering with the dark Higgs.

4.2 Higgs portal

The coupling $\lambda_{\Phi H}$ present in eq. (2.2) leads to mixing between the SM and dark Higgs, which enables a Higgs portal between the dark and visible sectors.

In the presence of Higgs-portal induced mixing between the SM and dark Higgs, the SM Higgs can decay invisibly into a pair of dark matter particles, with decay rate given by eq. (2.9):

$$\Gamma(h_2 \to XX) = \frac{3 \sin^2\theta m_{h_2}^3}{32\pi v_X^2} \left(1 - \frac{4m_X^2}{m_{h_2}^2} + \frac{12 m_X^4}{m_{h_2}^4} \right) \sqrt{1 - \frac{4m_X^2}{m_{h_2}^2}}. \tag{4.7}$$

The combined VBF, ZH and gluon fusion production of Higgs bosons at CMS leads to $\text{BR}(h_2 \to XX) < 0.24$ at 95% CL [50], while the ATLAS bounds from the VBF [51] and ZH [52] modes give $\text{BR}(h_2 \to XX) < 0.29$ and $\text{BR}(h_2 \to XX) < 0.75$, respectively. These decays provide a strong constraint on the mixing: $\sin\theta \lesssim 10^{-5}$ for $\alpha_X \sim \mathcal{O}(1)$.

The mixing also induces direct couplings of the darks Higgs to the SM electron and muons, which in turn induces tree-level scattering of the SM of the leptons. However, the smallness of the electron Yukawa coupling and the Boltzmann-suppression of the muons at the time of freezeout combined with constraints on the Higgs invisible decay result in the elastic scattering being inefficient for thermalization.

JHEP10(2017)162

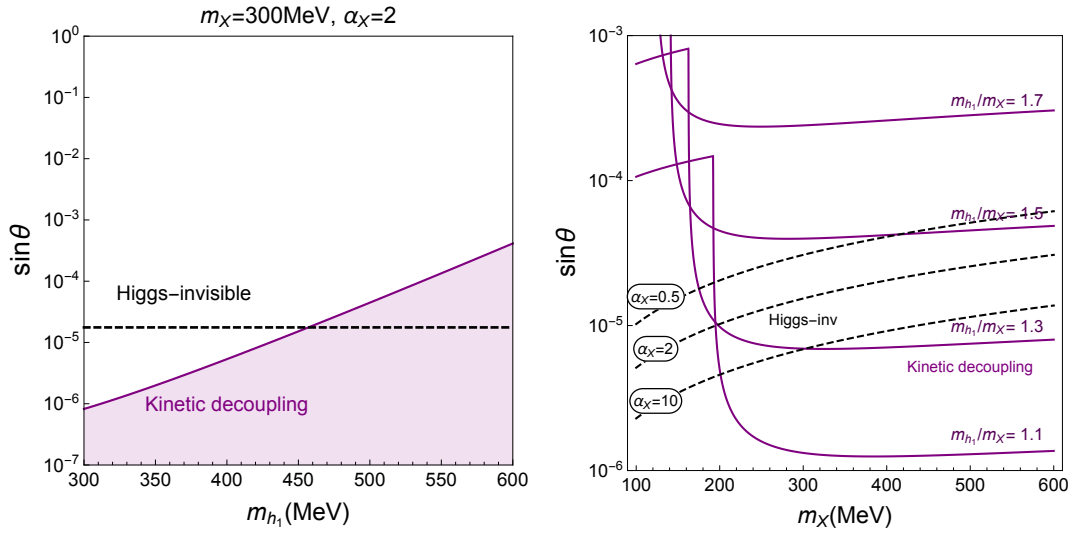

Figure 3. Vector SIMPs through the Higgs portal, with DM-dark Higgs scattering and dark Higgs-SM decays. *Left:* parameter space of m_{h_1} vs. $\sin\theta$ for DM-dark Higgs scattering. The shaded purple regions indicate where kinetic equilibrium between the DM and dark Higgs fails. *Right:* parameter space of m_X vs. $\sin\theta$. The purple lines are the lower bounds on $\sin\theta$ from kinetic equilibrium for fixed ratios m_{h_1}/m_X. *In both panels:* the dashed black curves are the upper bounds on $\sin\theta$ from Higgs invisible decays.

Alternatively, if the dark Higgs is fairly light, scattering between the vector dark matter and the dark Higgs can equilibrate the dark sector, with decays and inverse decays of the dark Higgs into SM particles completing the equilibration requirement between the SIMP and SM sectors. The momentum relaxation rate from the elastic scattering of dark matter off of dark Higgs, $X_i h_1 \to X_i h_1$, is given by

$$\gamma(T)_{h_1} = \frac{g_{h_1} g_X^4 m_{h_1}^2}{12\pi^3 m_X (m_X + m_{h_1})^2} \left(\frac{m_{h_1}^2 - 6m_X^2}{m_{h_1}^2 - 4m_X^2}\right)^2 T^2 \, e^{-m_{h_1}/T} \tag{4.8}$$

where $g_{h_1} = 1$. We note that the above result is valid for $m_{h_1}(m_{h_1} - 2m_X) \gtrsim p_{\rm DM}^2 \sim m_{\rm DM}^2 v_{\rm DM}^2$. Plugging this into the kinetic equilibrium condition eq. (4.5), we find that equilibrium between the dark Higgs and the DM is effective in most of parameter space satisfying the dark matter relic abundance.

Simultaneously, kinetic equilibrium between the dark Higgs and the SM is maintained by decays and the inverse decays of the Higgs into a pair of SM fermions,

$$\Gamma(h_1 \to f\bar{f}) = \frac{m_f^2 m_{h_1} \sin^2\theta}{8\pi v^2} \left(1 - \frac{4m_f^2}{m_{h_1}^2}\right)^{3/2} . \tag{4.9}$$

In figure 3, we illustrate this second requirement of equilibration between the dark Higgs and the SM, as a function of $\sin\theta$ and m_{h_1} (*left*) or m_X (*right*) for fixed m_X and α_X (*left*) or fixed ratio m_{h_1}/m_X (*right*). The upper bound on the mixing angle from invisible Higgs decays is indicated by the dashed black curves in both panels. Here the active thermalization process comes primarily from decays into muons when kinematically accessible, and from electrons for smaller masses.

JHEP10(2017)162

We learn that the Higgs portal is a viable mediator between vector SIMPs and the SM when the dark Higgs is close in mass to the DM. In this regime, $2 \to 2$ forbidden (semi)-annihilations channels of DM and the dark Higgs, $X_i X_j \to X_k h_1 (h_1 h_1)$, can be active and are then important contributors in determining the dark matter relic density, as discussed in section 3.2. In this case, the semi-annihilations are also active thermalization processes within the dark sector.

We note that current limits on Higgs mixing from rare kaon- and B-meson decays are weaker than the bound we impose from the Higgs invisible decay. However future beam dump or fixed target experiments, such as SHiP at CERN SPS, have the potential to probe the Higgs mixing angle further down [53]. The allowed parameter space for the Higgs portal to vector SIMPs could then be further probed as the invisible Higgs decay constraint improves.

Before ending this subsection, we remark that a Higgs portal coupling could allow in principle for the elastic scattering of relic vector SIMP dark matter with electrons in direct-detection experiments [54–64]. For $m_e, m_X, m_{Z'} \gg p_{\rm DM} \simeq m_X v_{\rm DM}$, the DM-electron direct detection scattering cross section via the Higgs portal is given by

$$\begin{aligned}\sigma_{\rm DD} &= \frac{\alpha_X \sin^2\theta \cos^2\theta m_e^4 m_X^2}{v^2 (m_e + m_X)^2} \left(\frac{1}{m_{h_1}^2} - \frac{1}{m_{h_2}^2}\right)^2 \\ &\approx 4 \times 10^{-50}\,{\rm cm}^2 \left(\frac{\alpha_X}{2}\right) \left(\frac{\sin\theta}{10^{-4}}\right)^2 \left(\frac{1.2}{m_{h_1}/m_X}\right)^4 \left(\frac{100\,{\rm MeV}}{m_X}\right)^4 . \end{aligned} \tag{4.10}$$

The small electron Yukawa coupling suppresses the cross section substantially, yielding a currently unconstrained spin-independent direct detection cross section.

4.3 Z' portal

Next, we explore the kinetically mixed Z' portal for mediation between the SIMP and visible sectors. We use the CS terms of eq. (2.15) to couple the vector DM to the Z', together with kinetic mixing between the Z' and the SM hypercharge. The momentum relaxation rate for vector DM scattering with electrons via the Z' portal is given by

$$\gamma(T)_{Z'} = \frac{1240\pi^3 c_1^2 e^2 \varepsilon^2}{567 m_X m_{Z'}^4} T^6 , \tag{4.11}$$

and one imposes eq. (4.5) for kinetic equilibrium.

The resulting allowed parameter space is depicted in figure 4 as a function of kinetic mixing ε, for fixed DM and Z' masses. The gray region is excluded by the unitarity bound on the CS term, and the kinetic equilibrium condition fails in the purple region. The LEP bound on the invisible decay width of the Z-boson, $\Gamma_{\rm inv} < 3\,{\rm MeV}$ [65] is shown in green, where we have assumed the dominant mode is into dark fermions that generate the CS coupling [as would be the case in generic UV completions with $N_f \alpha_{Z'} = 1$ in eq. (2.18)] in both plots. The BaBar constraint from invisible decays [66] is shown in blue (with a similar-sized constraint from the beam dump experiment NA64 at CERN SPS [69]).

In figure 5 we further show the allowed parameter space in ε and m_X (top panels) or $m_{Z'}$ (lower panels), for fixed values of the CS coefficient and of $m_{Z'}$ or m_X, respectively.

JHEP10(2017)162

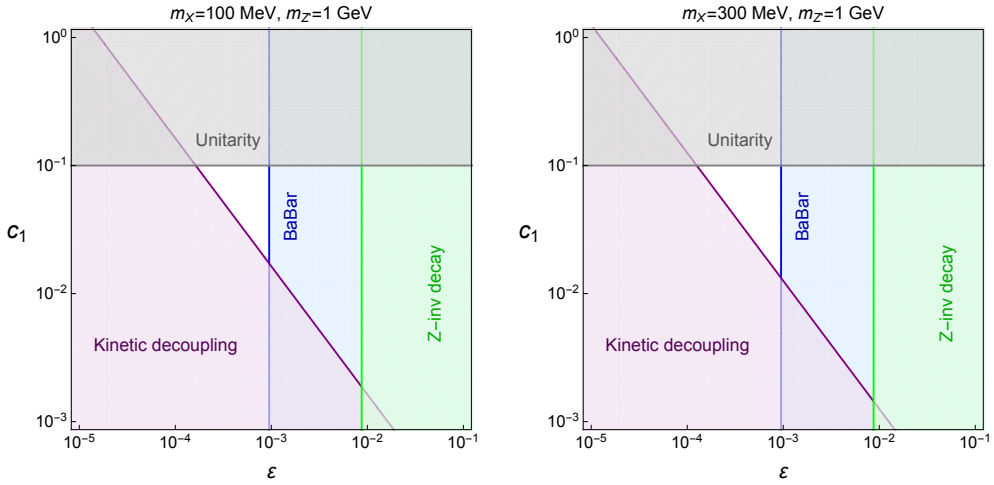

Figure 4. Allowed parameter space for vector SIMPs with a Z' portal in the ε and c_1 plane, for fixed values of DM and Z' masses. We show the bounds from unitarity (brown), kinetic equilibrium (purple), the invisible width of the Z boson (green) [65] and BaBar monophoton+MET (blue) [66]. Here, we took $N_f \alpha_{Z'} = 1$ in eq. (2.18) for Z-boson invisible decay bounds.

Here, kinetic equilibrium is not maintained in the purple region; $2 \to 2$ processes are dominant over $3 \to 2$ processes in the red region; invisible Z-decay limits [65] are imposed in green [where we have assumed the dominant mode is into dark fermions with $N_f \alpha_{Z'} = 1$ in eq. (2.18)]; and constraints from BaBar invisible [66] and visible [67] searches are shown in blue. The projected reach of Belle-II into the parameter space is shown in the dashed blue curve [68]. As is evident, vector SIMPs through the Z' portal can be achieved in an experimentally viable parameter space.

Concerning direct-detection, we note that the Z' portal coupling of vector SIMPs via the CS term gives rise to a p-wave velocity-suppressed elastic cross section off electrons. As a result, the spin-independent cross section between vector SIMPs and electrons via the Z' portal is highly suppressed, in contrast to the case of scalar SIMPs [15]. For $m_e, m_X, m_{Z'} \gg p_{\rm DM} \simeq m_X v_{\rm DM}$, the DM-electron scattering cross section with Z' portal is given by

$$\begin{aligned}\sigma_{\rm DD} &= \frac{16 c_1^2 \varepsilon^2 \alpha_{\rm em} m_e^2}{3 m_{Z'}^4} \frac{(m_X^2 + 2 m_e m_X - m_e^2) m_X^2}{(m_X + m_e)^4} v_{\rm DM}^2 \\ &\approx 6 \times 10^{-51}\,{\rm cm}^2 \left(\frac{c_1}{0.01}\right)^2 \left(\frac{\varepsilon}{10^{-3}}\right)^2 \left(\frac{500\,{\rm MeV}}{m_{Z'}}\right)^4 \left(\frac{v_{\rm DM}}{10^{-3}}\right)^2 . \end{aligned} \tag{4.12}$$

For illustration, contours of DM-electron scattering with $\sigma_{\rm DD} = 10^{-48\ (49)} {\rm cm}^2$ are depicted in the lower left (right) panel of figure 5.

We learn that a kinetically mixed Z' with CS couplings can successfully mediate interactions between the SIMP and SM sectors, consistent with all experimental constraints. We expect that future experiments such as Belle-II [68] and potentially measurements at LHCb [70] can further probe the allowed parameter space for vector SIMPs with a vector portal.

JHEP10(2017)162

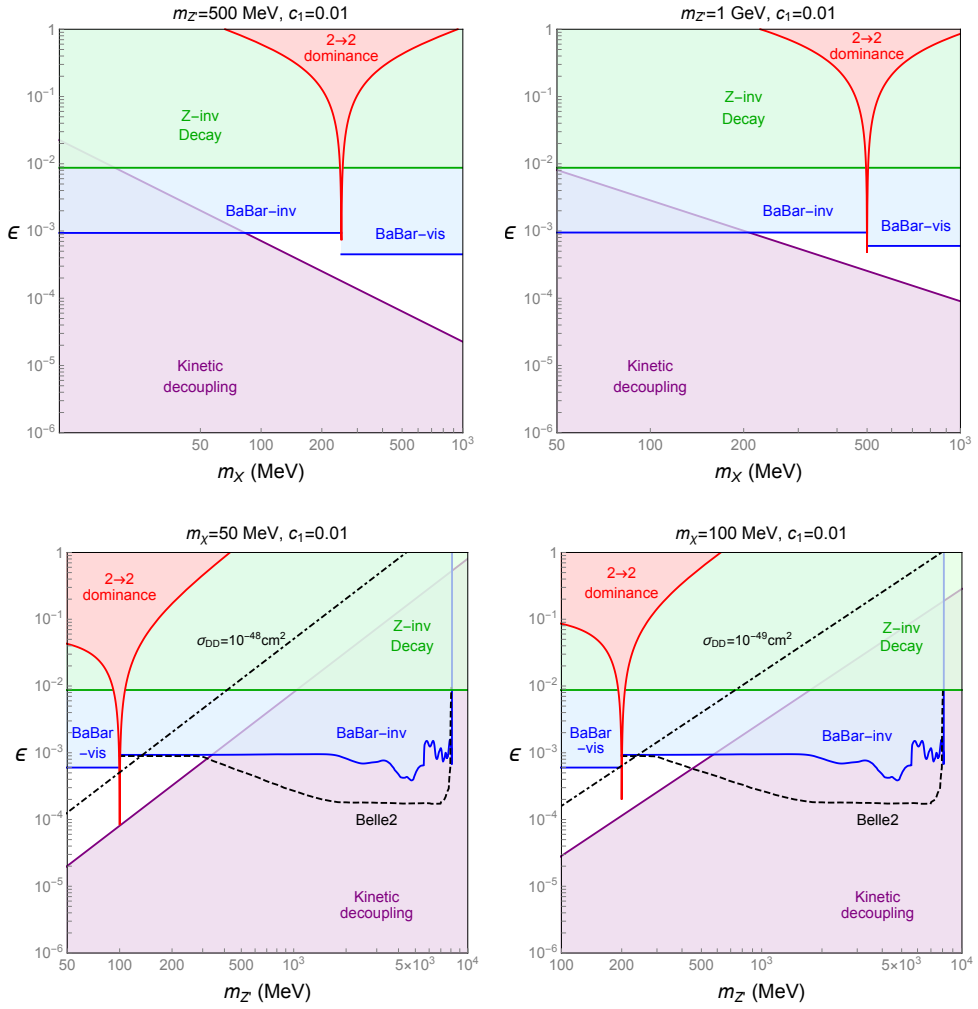

Figure 5. Allowed parameter space for vector SIMPs with a Z' portal. *Top:* parameter space of m_X vs. ε for $c_1 = 0.01$, for $m_{Z'} = 500\,\text{MeV}$ (*left*) and 1 GeV (*right*). *Bottom:* parameter space of $m_{Z'}$ vs. ε for $c_1 = 0.01$, for $m_X = 50\,\text{MeV}$ (*left*) and 100 MeV (*right*). Here, we took $N_f \alpha_{Z'} = 1$ in eq. (2.18) for the Z-boson invisible decay bound. *In all panels:* the purple region indicates where the kinetic equilibrium condition fails; the green region is excluded by the Z-boson invisible decay [65]; and the red region is where the $2 \to 2$ annihilation becomes dominant. BaBar searches for monophotons with MET [66] and with dileptons [67] exclude the blue region. The projected Belle-II reach for monophoton+MET [68] is depicted in dashed blue curve. Contours for DM-electron scattering cross section with $\sigma_{\rm DD} = 10^{-48\ (49)}\text{cm}^2$ are also shown in dot-dashed lines on the left (right) panels.

5 Conclusions

We have considered a spontaneously broken $\text{SU}(2)_X$ gauge theory in the hidden sector as an economical realization of vector SIMP dark matter. Kinetic equilibrium between the dark and visible sectors can be obtained via a Higgs portal in a minimal model or through a Z'-portal in an extended model with an additional $\text{U}(1)_{Z'}$ and its non-abelian Chern-Simons term. We have identified the parameter space for the $\text{SU}(2)_X$ gauge coupling and dark matter mass by taking into account the observed relic density as well as the self-scattering cross section. The kinetic equilibrium condition in combination with a variety

JHEP10(2017)162

of experimental constraints restrain the Higgs mixing or gauge kinetic mixing to a region that could be probed in current and planned experiments at the intensity frontiers.

Acknowledgments

The work of HML and SMC is supported in part by Basic Science Research Program through the National Research Foundation of Korea (NRF) funded by the Ministry of Education, Science and Technology (NRF-2016R1A2B4008759). The work of SMC is supported in part by TJ Park Science Fellowship of POSCO TJ Park Foundation. The work of YH is supported by the U.S. National Science Foundation, grant NSF-PHY-1419008, the LHC Theory Initiative, and by the Azrieli Foundation. EK is supported in part by the NSF under Grant No. PHY-1316222, and by a Hans Bethe Postdoctoral Fellowship at Cornell. EK would like to thank the Korea Institute for Advanced Study for hospitality, where the collaboration was initiated. YH and EK thank the Mainz Institute for Theoretical Physics for hospitality during the completion of this work. MP and YM want to thank the Spanish MICINN's Consolider-Ingenio 2010 Programme under grant Multi-Dark CSD2009-00064, the contract FPA2010-17747, the France-US PICS no. 06482 , partial support from the European Union's Horizon 2020 research and innovation programme (under the Marie Sklodowska-Curie grant agreements No 690575 and No 674896), and the ERC advanced grants. HM was supported by the U.S. DOE under Contract DE-AC02-05CH11231, and by the NSF under grants PHY-1316783 and PHY-1638509. HM was also supported by the JSPS Grant-in-Aid for Scientific Research (C) (No. 26400241 and 17K05409), MEXT Grant-in-Aid for Scientific Research on Innovative Areas (No. 15H05887, 15K21733), and by WPI, MEXT, Japan. HM also thanks Dorota Grabowska for useful discussions.

A The Chern Simons term

In this section, we discuss the origin of the generalized CS terms in a concrete model with dark fermions for a UV completion. Furthermore, we show that the effective CS terms and the general $Z' - X - X$ interactions can be derived from manifestly gauge invariant operators at low energy.

Suppose that there is a set of light fermions charged under $\mathrm{SU}(2)_X \times \mathrm{U}(1)_{Z'}$ such as

$$l = (2, +1), \quad \tilde{l} = (2, +1), \quad e^c = (1, -1), \quad \tilde{e}^c = (1, -1). \tag{A.1}$$

along with a heavy dark fermions with opposite $\mathrm{U}(1)_{Z'}$ charges $(L, \tilde{L}, E^c, \tilde{E}^c)$ that cancel the anomalies. With dark Higgs fields of charges $\Phi = (2, 0)$ and $S = (1, -2)$, then SU(2) vector-like and chiral masses from terms

$$S\, l\, \tilde{l} + S^* e^c\, \tilde{e}^c + \Phi\, l\, e^c + \tilde{\Phi}\, \tilde{l}\, \tilde{e}^c \tag{A.2}$$

where $\tilde{\Phi} = i\tau^2 \Phi^*$, are generated after $\mathrm{SU}(2)_X \times \mathrm{U}(1)_{Z'}$ spontaneous symmetry breaking.[1]

[1]The $\mathrm{SU}(2)_X$ gauge bosons masses are degenerate at tree level and receive small loop corrections due to the mass splitting between the members of each doublet fermion, that is proportional to chiral fermion mass. If the mass splitting between $\mathrm{SU}(2)_X$ gauge bosons is smaller than 10% of DM mass, all the SIMP processes are still active and dominant and the vector dark matter remains stable for heavy fermions. One can check explicitly in the example with vector-like dark fermions that there is no $X_3 - Z'$ mixing generated at loop level, so there is no issue of dark matter instability.

JHEP10(2017)162

When integrating out the light fermions, the non-decoupling portion of the one-loop triangle diagrams gives an effective CS term

$$\mathcal{L}_{\rm CS,EFT} = \frac{N_f g_{Z'} \alpha_X}{4\pi} \frac{m_X^2}{m_f^2} \epsilon^{\mu\nu\rho\sigma} Z'_\mu \vec{X}_\nu \cdot (\partial_\rho \vec{X}_\sigma - \partial_\sigma \vec{X}_\rho) \,, \tag{A.3}$$

where N_f being the number and mass of light fermion generations of mass, m_f. For instance, for $\alpha_X = 1(4)$, $N_f = 4(1)$, $g_{Z'} \sim 0.3$–3, and $m_f \sim 4m_X$–$10m_X$, we find the coefficient of the operator of eq. (2.15), $c_1 \simeq 0.01$. Therefore, for $m_f \gtrsim m_X$, we can avoid additional $2 \to 2$ annihilations of vector dark matter into light dark fermions, such as $XX \to f\bar{f}$, and a sizable CS term required for kinetic equilibrium can be consistently realized.

Notice here that the values of $c_1 \gtrsim 10^{-2}$ required for achieving the correct relic density in this setup imply a large multiplicity of the dark fermions or sizable gauge couplings which might drive the theory toward its non perturbative regime or the unstability of the dark higgs potential vacuum for energies of the order of the GeV scale. One could invoke more elaborate mechanisms in order to solve this potential issues but those are beyond the phenomenological considerations of this work.

If one considers only the light fermions $l = (2, +1), e^c = (1, -1)$ and their heavy partners for anomaly cancellation, then are only chiral fermion masses due to the $\mathrm{SU}(2)_X$ breaking. In this case, the needed CS terms are not generated. Instead, a nonzero dimension-6 interaction

$$\mathcal{L}_{D6} = \frac{c_3}{M^2} \epsilon^{\mu\mu\rho\sigma} \partial^\lambda Z'_{\mu\nu} (X_{1,\rho\sigma} X_{2,\lambda} - X_{2,\rho\sigma} X_{1,\lambda}) \,, \tag{A.4}$$

appears, which can also be sufficient for equilibrating the two sectors

Similarly, the effective dimension-6 operator in eq. (A.4) can be derived from another gauge invariant dimension-8 operator,

$$\mathcal{L}_{D8} = \frac{1}{M^4} \epsilon^{\mu\nu\rho\sigma} (\Phi^\dagger X_{\mu\nu} D_\lambda \Phi) \partial^\lambda Z'_{\rho\sigma} \,. \tag{A.5}$$

Then, in both cases with dimension-6 and dimension-8 operators, after the $\mathrm{SU}(2)_X$ is broken by the VEV of the scalar doublet Φ, the needed $Z'XX$ interactions are generated.

The effective approach considered in this work would be valid only for processes involving energies below the lightest dark fermion mass. Our approach is then justified for the DM freeze-out process which occurs when the DM becomes non-relativistic (i.e. for processes occuring at energies $\sim m_X \ll m_f$) and the dark fermions have already decoupled for the thermal bath. However, considering the invisible decay of the Z boson leads the effective approach to fail and one has to consider the complete dark fermions degrees of freedom in the computation.

JHEP10(2017)162

B Thermally averaged cross sections

After spin average for initial states and spin sum for the final states, the $2 \to 2$ self-scattering cross sections for vector dark matter (with notations, $ij \to ij$ meaning that $X_i X_j \to X_i X_j$, etc.), are in the non-relativistic limit

$$\sigma_{ii\to ii} = \frac{g_X^4 m_X^2 (15 m_{h_1}^4 - 80 m_{h_1}^2 m_X^2 + 128 m_X^4)}{384\pi m_{h_1}^4 (m_{h_1}^2 - 4m_X^2)^2}, \tag{B.1}$$

$$\sigma_{ij\to ij} = \frac{g_X^4}{192\pi m_{h_1}^4 m_X^2} (44 m_{h_1}^4 - 16 m_{h_1}^2 m_X^2 + 3 m_X^4), \quad i \neq j, \tag{B.2}$$

$$\sigma_{ii\to jj} = \frac{g_X^4 (172 m_{h_1}^4 - 1368 m_{h_1}^2 m_X^2 + 2723 m_X^4)}{384\pi m_X^2 (m_{h_1}^2 - 4m_X^2)^2}, \qquad i \neq j. \tag{B.3}$$

We define the thermal average for $2 \to 2$ annihilation, $\phi_1\phi_2 \to \phi_3\phi_4$, as follows,

$$\langle \sigma v \rangle = \frac{1}{n_1^{\rm eq} n_2^{\rm eq}} \frac{1}{s_i s_f} \int d\Pi_1 d\Pi_2 d\Pi_3 d\Pi_4 f_1^{\rm eq} f_2^{\rm eq} (2\pi)^4 \delta^4(p) |\mathcal{M}_{2\to 2}|^2 \tag{B.4}$$

where $n_{1,2}^{\rm eq}$, $f_{1,2}^{\rm eq}$ are the number densities and occupancies of particle $1, 2$ in thermal equilibrium, and $s_{i,f}$ are the symmetry factors for the initial or final states, which are $s_{i,f} = 1(2)$ for two identical (different) particles, and $d\Pi_i$ are the full phase space integrals for each particle, and $|\mathcal{M}_{2\to 2}|^2$ is the squared amplitude for $\phi_1\phi_2 \to \phi_3\phi_4$. Then, the $2 \to 2$ forbidden (semi-)annihilation cross sections (with notations, $h_1 h_1 \to ii$ meaning that $h_1 h_1 \to X_i X_i$ and $i h_1 \to jk$ meaning that $X_i h_1 \to X_j X_k$) are also given by

$$\begin{aligned}
\langle \sigma v \rangle_{h_1 h_1 \to ii} = {} & \frac{m_{h_1}^2}{512\pi m_X^4} \sqrt{1 - \frac{m_X^2}{m_{h_1}^2}} \left[64\lambda_\phi^2 \frac{m_X^4}{m_{h_1}^4} \left(4 - 4\frac{m_X^2}{m_{h_1}^2} + 3\frac{m_X^4}{m_{h_1}^4} \right) \right. \\
& - 16 g_X^2 \lambda_\phi \frac{m_X^2}{m_{h_1}^2} \left(4 + 8\frac{m_X^2}{m_{h_1}^2} - 15\frac{m_X^4}{m_{h_1}^4} + 12\frac{m_X^6}{m_{h_1}^6} \right) \\
& \left. + g_X^4 \left(4 + 20\frac{m_X^2}{m_{h_1}^2} + 11\frac{m_X^4}{m_{h_1}^4} - 56\frac{m_X^6}{m_{h_1}^6} + 48\frac{m_X^8}{m_{h_1}^8} \right) \right],
\end{aligned} \tag{B.5}$$

$$\begin{aligned}
\langle \sigma v \rangle_{i h_1 \to jk} = {} & \frac{g_X^4 m_{h_1}^3}{384\pi m_X^5} \left(1 + 3\frac{m_X}{m_{h_1}} \right)^{3/2} \left(1 - \frac{m_X}{m_{h_1}} \right)^{3/2} \left(1 + \frac{m_X}{m_{h_1}} \right)^{-1} \left(1 + 2\frac{m_X}{m_{h_1}} \right)^{-2} \\
& \times \left(1 + 4\frac{m_X}{m_{h_1}} - 4\frac{m_X^2}{m_{h_1}^2} - 10\frac{m_X^3}{m_{h_1}^3} + 144\frac{m_X^4}{m_{h_1}^4} + 396\frac{m_X^5}{m_{h_1}^5} + 297\frac{m_X^6}{m_{h_1}^6} \right)
\end{aligned} \tag{B.6}$$

with $i \neq j \neq k$ in the latter case.

We define the thermal average for $3 \to 2$ annihilation, $\phi_1\phi_2\phi_3 \to \phi_3\phi_4$, as follows,

$$\langle \sigma v^2 \rangle = \frac{1}{n_1^{\rm eq} n_2^{\rm eq} n_3^{\rm eq}} \frac{1}{s_i s_f} \int d\Pi_1 d\Pi_2 d\Pi_3 d\Pi_4 d\Pi_5 f_1^{\rm eq} f_2^{\rm eq} f_3^{\rm eq} (2\pi)^4 \delta^4(p) |\mathcal{M}_{3\to 2}|^2 \tag{B.7}$$

where $s_{i,f}$ are the symmetry factors, which are given by $s_i = n_i!$ and $s_f = n_f!$, depending on the number of identical particles in the initial and final states, n_i and n_f, respectively, and $|\mathcal{M}_{3\to 2}|^2$ is the squared amplitude for $\phi_1\phi_2\phi_3 \to \phi_4\phi_5$.

JHEP10(2017)162

The $3 \to 2$ annihilation cross sections including only $SU(2)_X$ gauge interactions (with notations, $123 \to 11$ meaning $X_1X_2X_3 \to X_1X_1$, etc) are, in the non-relativistic limit,

$$\begin{aligned}
\langle\sigma v^2\rangle_{ijk} &\equiv \langle\sigma v^2\rangle_{123\to 11} = \langle\sigma v^2\rangle_{123\to 22} = \langle\sigma v^2\rangle_{123\to 33} \\
&= \frac{5\sqrt{5}g_X^6}{331776\pi m_X^5(m_{h_1}^2+m_X^2)^2}\left(347m_{h_1}^4+586m_{h_1}^2m_X^2+707m_X^4\right) \\
&\quad + \frac{19\sqrt{5}g_X^6}{1152\pi m_X(9m_X^2-m_{h_1}^2)^2}\left\langle(v_1^2+v_2^2+v_1v_2\cos\theta_{12})\right\rangle, \qquad \text{(B.8)} \\
\langle\sigma v^2\rangle_{iij} &\equiv \langle\sigma v^2\rangle_{112\to 13} = \langle\sigma v^2\rangle_{113\to 12} = \langle\sigma v^2\rangle_{221\to 23} = \langle\sigma v^2\rangle_{223\to 12} \\
&= \langle\sigma v^2\rangle_{331\to 23} = \langle\sigma v^2\rangle_{332\to 13} \\
&= \frac{5\sqrt{5}g_X^6}{2654208\pi m_X^5}\left(14377+\frac{6m_X^2(157m_{h_1}^2-763m_X^2)}{(m_{h_1}^2-4m_X^2)(m_{h_1}^2+m_X^2)}\right. \\
&\quad \left. + \frac{3m_X^4(5281m_{h_1}^4-18558m_{h_1}^2m_X^2+32561m_X^4)}{(m_{h_1}^2-4m_X^2)^2(m_{h_1}^2+m_X^2)^2}\right), \qquad \text{(B.9)} \\
\langle\sigma v^2\rangle_{iii} &= \langle\sigma v^2\rangle_{111\to 23} = \langle\sigma v^2\rangle_{222\to 13} = \langle\sigma v^2\rangle_{333\to 12} \\
&= \frac{25\sqrt{5}g_X^6}{2654208\pi m_X^5}\left(8375+\frac{362m_X^2}{m_{h_1}^2-4m_X^2}+\frac{1713m_X^4}{(m_{h_1}^2-4m_X^2)^2}\right). \qquad \text{(B.10)}
\end{aligned}$$

Here, we have included the p-wave terms in $\langle\sigma v^2\rangle_{iii}$ as they have a resonance at $m_{h_1} = 3m_X$. We note that v_1, v_2 are the speeds of two dark matter particles in the initial states and θ_{12} is the angle between the two in the center of mass frame.

On the other hand, the $3 \to 2$ annihilation cross sections including the dark Higgs (with notations, $122 \to 1h_1$ meaning $X_1X_2X_2 \to X_1h_1$, etc) are, in the non-relativistic limit,

$$\begin{aligned}
\langle\sigma v^2\rangle_{iii}^h &\equiv \langle\sigma v^2\rangle_{111\to 1h_1} = \langle\sigma v^2\rangle_{222\to 2h_1} = \langle\sigma v^2\rangle_{333\to 3h_1} \\
&= \frac{\sqrt{5}g_X^6 m_{h_1}^{16}C_1(1-m_{h_1}^2/(16m_X^2))^{1/2}}{17915904\pi m_X^{10}(4m_X^2-m_{h_1}^2)^{7/2}(2m_X^2+m_{h_1}^2)^2} \qquad \text{(B.11)}
\end{aligned}$$

with

$$\begin{aligned}
C_1 \equiv \frac{1}{m_{h_1}^{16}}\Big(&3m_{h_1}^{16}-270m_{h_1}^{14}m_X^2+9917m_{h_1}^{12}m_X^4-187056m_{h_1}^{10}m_X^6+1952400m_{h_1}^8m_X^8 \\
&-11318848m_{h_1}^6m_X^{10}+35045232m_{h_1}^4m_X^{12}-52110336m_{h_1}^2m_X^{14}+30261248m_X^{16}\Big) \qquad \text{(B.12)}
\end{aligned}$$

and

$$\begin{aligned}
\langle\sigma v^2\rangle_{ijj}^h &\equiv \langle\sigma v^2\rangle_{122\to 1h_1} = \langle\sigma v^2\rangle_{133\to 1h_1} = \langle\sigma v^2\rangle_{211\to 2h_1} = \langle\sigma v^2\rangle_{233\to 2h_1} \\
&= \langle\sigma v^2\rangle_{311\to 3h_1} = \langle\sigma v^2\rangle_{322\to 3h_1} \\
&= \frac{\sqrt{5}g_X^6 m_{h_1}^{20}C_2(1-m_{h_1}^2/(16m_X^2))^{1/2}}{17915904\pi m_X^{10}(4m_X^2-m_{h_1}^2)^{7/2}(2m_X^2+m_{h_1}^2)^2(7m_X^2-m_{h_1}^2)^2} \qquad \text{(B.13)}
\end{aligned}$$

JHEP10(2017)162

with

$$C_2 \equiv \frac{1}{m_{h_1}^{20}}\Big(13m_{h_1}^{20} - 568m_{h_1}^{18}m_X^2 + 33204m_{h_1}^{16}m_X^4 - 724140m_{h_1}^{14}m_X^6 + 6743931m_{h_1}^{12}m_X^8 - 26087280m_{h_1}^{10}m_X^{10} + 48284736m_{h_1}^{8}m_X^{12} - 166749984m_{h_1}^{6}m_X^{14} + 806289168m_{h_1}^{4}m_X^{16} - 2275720192m_{h_1}^{2}m_X^{18} + 3442229248m_X^{20}\Big). \tag{B.14}$$

We note that the factor $1/(4m_X^2 - m_{h_1}^2)^4$ in the above results is the squared product of the dark Higgs propagator in s-channel and the dark matter propagator in t-channel, which are regularized at $m_{h_1} = 2m_X$ by the finite width of the dark Higgs and a nonzero dark matter velocity, respectively. The $3 \to 2$ annihilation cross sections including two dark Higgs bosons such as $XXX \to h_1 h_1$ are p-wave suppressed and sub-dominant, so we don't include them here.

The Boltzmann equation for the total DM density $n_{\rm DM}$ is

$$\begin{aligned}\frac{dn_{\rm DM}}{dt} + 3Hn_{\rm DM} = &-\frac{2}{3}\langle\sigma v\rangle_{ii}(n_{\rm DM}^2 - (n_{\rm DM}^{\rm eq})^2) \\ &- \frac{1}{9}\Big(\langle\sigma v^2\rangle_{ijk} + 2\langle\sigma v^2\rangle_{iij} + \langle\sigma v^2\rangle_{iii}\Big)(n_{\rm DM}^3 - n_{\rm DM}^2 n_{\rm DM}^{\rm eq}) \\ &- \frac{2}{9}\Big(\langle\sigma v^2\rangle_{iii}^h + 2\langle\sigma v^2\rangle_{ijj}^h\Big)(n_{\rm DM}^3 - n_{\rm DM}(n_{\rm DM}^{\rm eq})^2) \\ &- \frac{2}{3}\langle\sigma v\rangle_{ii\to h_1h_1} n_{\rm DM}^2 + 6\langle\sigma v\rangle_{h_1h_1\to ii}(n_{h_1}^{\rm eq})^2 \\ &- \frac{1}{3}\langle\sigma v\rangle_{ij\to kh_1} n_{\rm DM}^2 + \langle\sigma v\rangle_{kh_1\to ij} n_{h_1}^{\rm eq} n_{\rm DM}.\end{aligned} \tag{B.15}$$

Here, we have assumed that h_1 maintains chemical and thermal equilibrium with the SM bath throughout freezeout. We note that $\langle\sigma v\rangle_{ii}$ in the first line is the averaged $2 \to 2$ annihilation cross section into a pair of the SM fermions, i.e. $X_i X_i \to f\bar{f}$.

References

[1] Planck collaboration, P.A.R. Ade et al., *Planck 2015 results. XIII. Cosmological parameters*, *Astron. Astrophys.* **594** (2016) A13 [arXiv:1502.01589] [inSPIRE].

[2] G. Arcadi et al., *The Waning of the WIMP? A Review of Models, Searches and Constraints*, arXiv:1703.07364 [inSPIRE].

[3] XENON100 collaboration, E. Aprile et al., *XENON100 Dark Matter Results from a Combination of 477 Live Days*, *Phys. Rev.* **D 94** (2016) 122001 [arXiv:1609.06154] [inSPIRE].

[4] LUX collaboration, D.S. Akerib et al., *Results from a search for dark matter in the complete LUX exposure*, *Phys. Rev. Lett.* **118** (2017) 021303 [arXiv:1608.07648] [inSPIRE].

JHEP10(2017)162

[5] PandaX-II collaboration, A. Tan et al., *Dark Matter Results from First 98.7 Days of Data from the PandaX-II Experiment*, *Phys. Rev. Lett.* **117** (2016) 121303 [arXiv:1607.07400] [INSPIRE].

[6] Fermi-LAT collaboration, M. Ackermann et al., *Limits on Dark Matter Annihilation Signals from the Fermi LAT 4-year Measurement of the Isotropic Gamma-Ray Background*, *JCAP* **09** (2015) 008 [arXiv:1501.05464] [INSPIRE].

[7] H.E.S.S. collaboration, H. Abdallah et al., *Search for dark matter annihilations towards the inner Galactic halo from 10 years of observations with H.E.S.S*, *Phys. Rev. Lett.* **117** (2016) 111301 [arXiv:1607.08142] [INSPIRE].

[8] J.L. Feng and J. Kumar, *The WIMPless Miracle: Dark-Matter Particles without Weak-Scale Masses or Weak Interactions*, *Phys. Rev. Lett.* **101** (2008) 231301 [arXiv:0803.4196] [INSPIRE].

[9] E.D. Carlson, M.E. Machacek and L.J. Hall, *Self-interacting dark matter*, *Astrophys. J.* **398** (1992) 43 [INSPIRE].

[10] Y. Hochberg, E. Kuflik, T. Volansky and J.G. Wacker, *Mechanism for Thermal Relic Dark Matter of Strongly Interacting Massive Particles*, *Phys. Rev. Lett.* **113** (2014) 171301 [arXiv:1402.5143] [INSPIRE].

[11] Y. Hochberg, E. Kuflik, H. Murayama, T. Volansky and J.G. Wacker, *Model for Thermal Relic Dark Matter of Strongly Interacting Massive Particles*, *Phys. Rev. Lett.* **115** (2015) 021301 [arXiv:1411.3727] [INSPIRE].

[12] K. Griest and D. Seckel, *Three exceptions in the calculation of relic abundances*, *Phys. Rev.* **D 43** (1991) 3191 [INSPIRE].

[13] R.T. D'Agnolo and J.T. Ruderman, *Light Dark Matter from Forbidden Channels*, *Phys. Rev. Lett.* **115** (2015) 061301 [arXiv:1505.07107] [INSPIRE].

[14] H.M. Lee and M.-S. Seo, *Communication with SIMP dark mesons via Z'-portal*, *Phys. Lett.* **B 748** (2015) 316 [arXiv:1504.00745] [INSPIRE].

[15] S.-M. Choi and H.M. Lee, *SIMP dark matter with gauged Z_3 symmetry*, *JHEP* **09** (2015) 063 [arXiv:1505.00960] [INSPIRE].

[16] Y. Hochberg, E. Kuflik and H. Murayama, *SIMP Spectroscopy*, *JHEP* **05** (2016) 090 [arXiv:1512.07917] [INSPIRE].

[17] S.-M. Choi and H.M. Lee, *Resonant SIMP dark matter*, *Phys. Lett.* **B 758** (2016) 47 [arXiv:1601.03566] [INSPIRE].

[18] S.-M. Choi, Y.-J. Kang and H.M. Lee, *On thermal production of self-interacting dark matter*, *JHEP* **12** (2016) 099 [arXiv:1610.04748] [INSPIRE].

[19] S.-M. Choi, H.M. Lee and M.-S. Seo, *Cosmic abundances of SIMP dark matter*, *JHEP* **04** (2017) 154 [arXiv:1702.07860] [INSPIRE].

[20] T. Hambye and M.H.G. Tytgat, *Confined hidden vector dark matter*, *Phys. Lett.* **B 683** (2010) 39 [arXiv:0907.1007] [INSPIRE].

[21] T. Hambye, *Hidden vector dark matter*, *JHEP* **01** (2009) 028 [arXiv:0811.0172] [INSPIRE].

[22] A. Karam and K. Tamvakis, *Dark matter and neutrino masses from a scale-invariant multi-Higgs portal*, *Phys. Rev.* **D 92** (2015) 075010 [arXiv:1508.03031] [INSPIRE].

JHEP10(2017)162

[23] A. Karam and K. Tamvakis, *Dark Matter from a Classically Scale-Invariant* $SU(3)_X$, *Phys. Rev.* **D 94** (2016) 055004 [arXiv:1607.01001] [INSPIRE].

[24] N. Bernal, X. Chu, C. Garcia-Cely, T. Hambye and B. Zaldivar, *Production Regimes for Self-Interacting Dark Matter*, *JCAP* **03** (2016) 018 [arXiv:1510.08063] [INSPIRE].

[25] M. Heikinheimo, T. Tenkanen and K. Tuominen, *WIMP miracle of the second kind*, *Phys. Rev.* **D 96** (2017) 023001 [arXiv:1704.05359] [INSPIRE].

[26] J. Cline, H. Liu, T. Slatyer and W. Xue, *Enabling Forbidden Dark Matter*, arXiv:1702.07716 [INSPIRE].

[27] U.K. Dey, T.N. Maity and T.S. Ray, *Light Dark Matter through Assisted Annihilation*, *JCAP* **03** (2017) 045 [arXiv:1612.09074] [INSPIRE].

[28] A. Kamada, M. Yamada, T.T. Yanagida and K. Yonekura, *SIMP from a strong U(1) gauge theory with a monopole condensation*, *Phys. Rev.* **D 94** (2016) 055035 [arXiv:1606.01628] [INSPIRE].

[29] O. Lebedev, H.M. Lee and Y. Mambrini, *Vector Higgs-portal dark matter and the invisible Higgs*, *Phys. Lett.* **B 707** (2012) 570 [arXiv:1111.4482] [INSPIRE].

[30] P. Anastasopoulos, M. Bianchi, E. Dudas and E. Kiritsis, *Anomalies, anomalous U(1)'s and generalized Chern-Simons terms*, *JHEP* **11** (2006) 057 [hep-th/0605225] [INSPIRE].

[31] I. Antoniadis, A. Boyarsky, S. Espahbodi, O. Ruchayskiy and J.D. Wells, *Anomaly driven signatures of new invisible physics at the Large Hadron Collider*, *Nucl. Phys.* **B 824** (2010) 296 [arXiv:0901.0639] [INSPIRE].

[32] Y. Mambrini, *A Clear Dark Matter gamma ray line generated by the Green-Schwarz mechanism*, *JCAP* **12** (2009) 005 [arXiv:0907.2918] [INSPIRE].

[33] E. Dudas, Y. Mambrini, S. Pokorski and A. Romagnoni, *(In)visible Z-prime and dark matter*, *JHEP* **08** (2009) 014 [arXiv:0904.1745] [INSPIRE].

[34] H.M. Lee, D. Kim, K. Kong and S.C. Park, *Diboson Excesses Demystified in Effective Field Theory Approach*, *JHEP* **11** (2015) 150 [arXiv:1507.06312] [INSPIRE].

[35] G. Arcadi, P. Ghosh, Y. Mambrini, M. Pierre and F.S. Queiroz, *Z' portal to Chern-Simons Dark Matter*, arXiv:1706.04198 [INSPIRE].

[36] G. 't Hooft, *Which Topological Features of a Gauge Theory Can Be Responsible for Permanent Confinement?*, *NATO Sci. Ser.* **B 59** (1980) 117 [INSPIRE].

[37] E. D'Hoker and E. Farhi, *Decoupling a Fermion Whose Mass Is Generated by a Yukawa Coupling: The General Case*, *Nucl. Phys.* **B 248** (1984) 59 [INSPIRE].

[38] D. Clowe, A. Gonzalez and M. Markevitch, *Weak lensing mass reconstruction of the interacting cluster 1E0657-558: Direct evidence for the existence of dark matter*, *Astrophys. J.* **604** (2004) 596 [astro-ph/0312273] [INSPIRE].

[39] M. Markevitch et al., *Direct constraints on the dark matter self-interaction cross-section from the merging galaxy cluster 1E0657-56*, *Astrophys. J.* **606** (2004) 819 [astro-ph/0309303] [INSPIRE].

[40] S.W. Randall, M. Markevitch, D. Clowe, A.H. Gonzalez and M. Bradac, *Constraints on the Self-Interaction Cross-Section of Dark Matter from Numerical Simulations of the Merging Galaxy Cluster 1E 0657-56*, *Astrophys. J.* **679** (2008) 1173 [arXiv:0704.0261] [INSPIRE].

JHEP10(2017)162

[41] M. Rocha et al., *Cosmological Simulations with Self-Interacting Dark Matter I: Constant Density Cores and Substructure*, *Mon. Not. Roy. Astron. Soc.* **430** (2013) 81 [arXiv:1208.3025] [INSPIRE].

[42] A.H.G. Peter, M. Rocha, J.S. Bullock and M. Kaplinghat, *Cosmological Simulations with Self-Interacting Dark Matter II: Halo Shapes vs. Observations*, *Mon. Not. Roy. Astron. Soc.* **430** (2013) 105 [arXiv:1208.3026] [INSPIRE].

[43] E.H. Fradkin and S.H. Shenker, *Phase Diagrams of Lattice Gauge Theories with Higgs Fields*, *Phys. Rev.* **D 19** (1979) 3682 [INSPIRE].

[44] T. Banks and E. Rabinovici, *Finite Temperature Behavior of the Lattice Abelian Higgs Model*, *Nucl. Phys.* **B 160** (1979) 349 [INSPIRE].

[45] L. Susskind, *Lattice Models of Quark Confinement at High Temperature*, *Phys. Rev.* **D 20** (1979) 2610 [INSPIRE].

[46] S. Raby, S. Dimopoulos and L. Susskind, *Tumbling Gauge Theories*, *Nucl. Phys.* **B 169** (1980) 373 [INSPIRE].

[47] H. Georgi, *Complementarity and Stability Conditions*, *Phys. Lett.* **B 771** (2017) 558 [arXiv:1607.00369] [INSPIRE].

[48] E. Kuflik, M. Perelstein, N. R.-L. Lorier and Y.-D. Tsai, *Elastically Decoupling Dark Matter*, *Phys. Rev. Lett.* **116** (2016) 221302 [arXiv:1512.04545] [INSPIRE].

[49] E. Kuflik, M. Perelstein, N. R.-L. Lorier and Y.-D. Tsai, *Phenomenology of ELDER Dark Matter*, *JHEP* **08** (2017) 078 [arXiv:1706.05381] [INSPIRE].

[50] CMS collaboration, *Searches for invisible decays of the Higgs boson in pp collisions at* $\sqrt{s} = 7, 8$ *and* 13 *TeV*, *JHEP* **02** (2017) 135 [arXiv:1610.09218] [INSPIRE].

[51] ATLAS collaboration, *Search for invisible decays of a Higgs boson using vector-boson fusion in pp collisions at* $\sqrt{s} = 8$ *TeV with the ATLAS detector*, *JHEP* **01** (2016) 172 [arXiv:1508.07869] [INSPIRE].

[52] ATLAS collaboration, *Search for Invisible Decays of a Higgs Boson Produced in Association with a Z Boson in ATLAS*, *Phys. Rev. Lett.* **112** (2014) 201802 [arXiv:1402.3244] [INSPIRE].

[53] S. Alekhin et al., *A facility to Search for Hidden Particles at the CERN SPS: the SHiP physics case*, *Rept. Prog. Phys.* **79** (2016) 124201 [arXiv:1504.04855] [INSPIRE].

[54] R. Essig, J. Mardon and T. Volansky, *Direct Detection of Sub-GeV Dark Matter*, *Phys. Rev.* **D 85** (2012) 076007 [arXiv:1108.5383] [INSPIRE].

[55] P.W. Graham, D.E. Kaplan, S. Rajendran and M.T. Walters, *Semiconductor Probes of Light Dark Matter*, *Phys. Dark Univ.* **1** (2012) 32 [arXiv:1203.2531] [INSPIRE].

[56] S.K. Lee, M. Lisanti, S. Mishra-Sharma and B.R. Safdi, *Modulation Effects in Dark Matter-Electron Scattering Experiments*, *Phys. Rev.* **D 92** (2015) 083517 [arXiv:1508.07361] [INSPIRE].

[57] R. Essig, M. Fernandez-Serra, J. Mardon, A. Soto, T. Volansky and T.-T. Yu, *Direct Detection of sub-GeV Dark Matter with Semiconductor Targets*, *JHEP* **05** (2016) 046 [arXiv:1509.01598] [INSPIRE].

[58] Y. Hochberg, Y. Zhao and K.M. Zurek, *Superconducting Detectors for Superlight Dark Matter*, *Phys. Rev. Lett.* **116** (2016) 011301 [arXiv:1504.07237] [INSPIRE].

[59] Y. Hochberg, M. Pyle, Y. Zhao and K.M. Zurek, *Detecting Superlight Dark Matter with Fermi-Degenerate Materials*, *JHEP* **08** (2016) 057 [arXiv:1512.04533] [INSPIRE].

JHEP10(2017)162

[60] Y. Hochberg, Y. Kahn, M. Lisanti, C.G. Tully and K.M. Zurek, *Directional detection of dark matter with two-dimensional targets*, *Phys. Lett.* **B 772** (2017) 239 [arXiv:1606.08849] [INSPIRE].

[61] R. Essig, J. Mardon, O. Slone and T. Volansky, *Detection of sub-GeV Dark Matter and Solar Neutrinos via Chemical-Bond Breaking*, *Phys. Rev.* **D 95** (2017) 056011 [arXiv:1608.02940] [INSPIRE].

[62] S. Derenzo, R. Essig, A. Massari, A. Soto and T.-T. Yu, *Direct Detection of sub-GeV Dark Matter with Scintillating Targets*, *Phys. Rev.* **D 96** (2017) 016026 [arXiv:1607.01009] [INSPIRE].

[63] J. Tiffenberg et al., *Single-electron and single-photon sensitivity with a silicon Skipper CCD*, *Phys. Rev. Lett.* **119** (2017) 131802 [arXiv:1706.00028] [INSPIRE].

[64] R. Essig, T. Volansky and T.-T. Yu, *New Constraints and Prospects for sub-GeV Dark Matter Scattering off Electrons in Xenon*, *Phys. Rev.* **D 96** (2017) 043017 [arXiv:1703.00910] [INSPIRE].

[65] ALEPH, DELPHI, L3, OPAL, SLD collaborations LEP Electroweak Working Group, SLD Electroweak Group, SLD Heavy Flavour Group, S. Schael et al., *Precision electroweak measurements on the Z resonance*, *Phys. Rept.* **427** (2006) 257 [hep-ex/0509008] [INSPIRE].

[66] BABAR collaboration, J.P. Lees et al., *Search for Invisible Decays of a Dark Photon Produced in e^+e^- Collisions at BaBar*, *Phys. Rev. Lett.* **119** (2017) 131804 [arXiv:1702.03327] [INSPIRE].

[67] BABAR collaboration, J.P. Lees et al., *Search for a Dark Photon in e^+e^- Collisions at BaBar*, *Phys. Rev. Lett.* **113** (2014) 201801 [arXiv:1406.2980] [INSPIRE].

[68] R. Essig, J. Mardon, M. Papucci, T. Volansky and Y.-M. Zhong, *Constraining Light Dark Matter with Low-Energy e^+e^- Colliders*, *JHEP* **11** (2013) 167 [arXiv:1309.5084] [INSPIRE].

[69] NA64 collaboration, D. Banerjee et al., *Search for invisible decays of sub-GeV dark photons in missing-energy events at the CERN SPS*, *Phys. Rev. Lett.* **118** (2017) 011802 [arXiv:1610.02988] [INSPIRE].

[70] P. Ilten, Y. Soreq, J. Thaler, M. Williams and W. Xue, *Proposed Inclusive Dark Photon Search at LHCb*, *Phys. Rev. Lett.* **116** (2016) 251803 [arXiv:1603.08926] [INSPIRE].

JHEP10(2017)162